Geological Quarterly, 2024, 68: 4
DOI: http://dx.doi.org/10.7306/gq.1727

A first record of alluvial gold in the Olăneşti and Chşeia rivers, Southern Carpathians, Romania

Sergiu DRĂGUŞANU[1], Călin Gabriel TĂMAŞ[1, *] and Mădălina Paula ANDRII[1]

[1] Babeş-Bolyai University, 1 Kogălniceanu, 400084 Cluj Napoca, Romania; ORCID: 0009-0009-2894-017X [SD], 0000-0002-1782-4714 [C.G.T.], 0000-0001-9619-7554 [M.P.A.]

Drăguşanu, S., Tămaş, C.T., Andrii, M.P., 2024. A first record of alluvial gold in the Olăneşti and Cheia rivers, Southern Carpathians, Romania. Geological Quarterly, 2024, 68: 4; https://doi.org/10.7306/gq.1727

Associate Editor: Stanisław Mikulski

We provide the first scientific record and the mineralogical characterization of alluvial gold in the Olăneşti area, Southern Carpathians, Romania, based on field evidence, optical microscopy, and XRD, BSE and EPMA data. Chemical data were acquired on 11 alluvial gold grains from the Olăneşti and Cheia rivers and revealed a generally continuous variation in gold and silver content with Ag ranging from 7.31 to 19.77 wt.% and Au ranging from 80.26 to 93.16 wt.%. The source of the primary native gold is inferred to be the Cu-Au Valea lui Stan and/or the Costşti As-Au shear-zone-related ore deposits located towards the north and west, respectively, of the study area.

Key words: alluvial gold, Olăneşti, Southern Carpathians.

INTRODUCTION

The territory of Romania has been known as a major gold source since at least Roman times, with an all-time gold production estimated at 1500–2000 tons by Cook and Ciobanu (2004). The most important gold production areas are the South Apuseni Mountains, more specifically, the "Golden Quadrilateral" area defined by Ghiţulescu and Socolescu (1941), and the Baia Mare ore district in the northwestern part of the Eastern Carpathians (Neubauer et al., 2005). The gold-bearing ores in both regions belong to the intermediate sulphidation and low sulphidation epithermal types with veins, breccias and stockworks such as the Roşia Montană and Săsar ore deposits. Apart from the primary gold deposits, five placer gold deposits are known in Romania: Pianu, Cibin-Olt Valley, Râureni, Arieş Valley and Nera/Bozovici (Borcoş et al., 1984). The best known is that of Pianu, where traces of the placer gold mining dating back to the 2nd and 3rd centuries CE are well-preserved (Cauuet et al., 1999; Bedelean and Bedelean, 2001). Additionally, three other alluvial gold occurrences along the Crişul Alb, Mureş and Strei rivers were noted by Galcenco et al. (1995) as being economically viable.

This paper reports a new alluvial gold occurrence in the Olăneşti area (Olăneşti and Cheia rivers) in Romania, and provides EPMA data on the gold grains.

GEOLOGICAL SETTING

The study area comprises the drainage basins of the Olăneşti and Cheia rivers (Fig. 1), located in the Căpăţânii Mountains, Southern Carpathians, Romania, which, together with the Eastern Carpathians and the Apuseni Mountains, form the Carpathian chain, a section of the Western Tethyan Alpine orogenic belt (Săndulescu, 1984; Balintoni, 1997; Schmid et al., 2008; Richards, 2015).

The Southern Carpathians comprise, from bottom to top, three main structural units (Balintoni, 1997; Iancu et al., 1998; Medaris et al., 2003): (i) the Danubian nappe system or Danubian Euxinides according to Balintoni (1997); (ii) the Severin and Arajna nappes or Euxinides according to Balintoni (1997); and (iii) the Getic-Supragetic nappe system (Median Dacides according to Săndulescu, 1984) or Getic Domain according to Balintoni (1997).

Our study focuses on the sedimentary cover of the Sebeş-Lotru pre-Alpine terranes, which form part of the Getic Domain (Balintoni et al., 2010). The Sebeş-Lotru terrane comprises the Neoproterozoic Lotru unit and above this the Ordovician Cumpăna Unit (Balintoni et al., 2010). These units consist of orthogneisses, granitoids, metabasites and metaultrabasites.

Lupu et al. (1978) stated that the sedimentary cover comprises Upper Jurassic limestones (Buila-Vânturariţa Massif) in

* Corresponding author, e-mail: calin.tamas@ubbcluj.ro
Received: July 20, 2023; accepted December 21, 2024; first published online: April 4, 2024

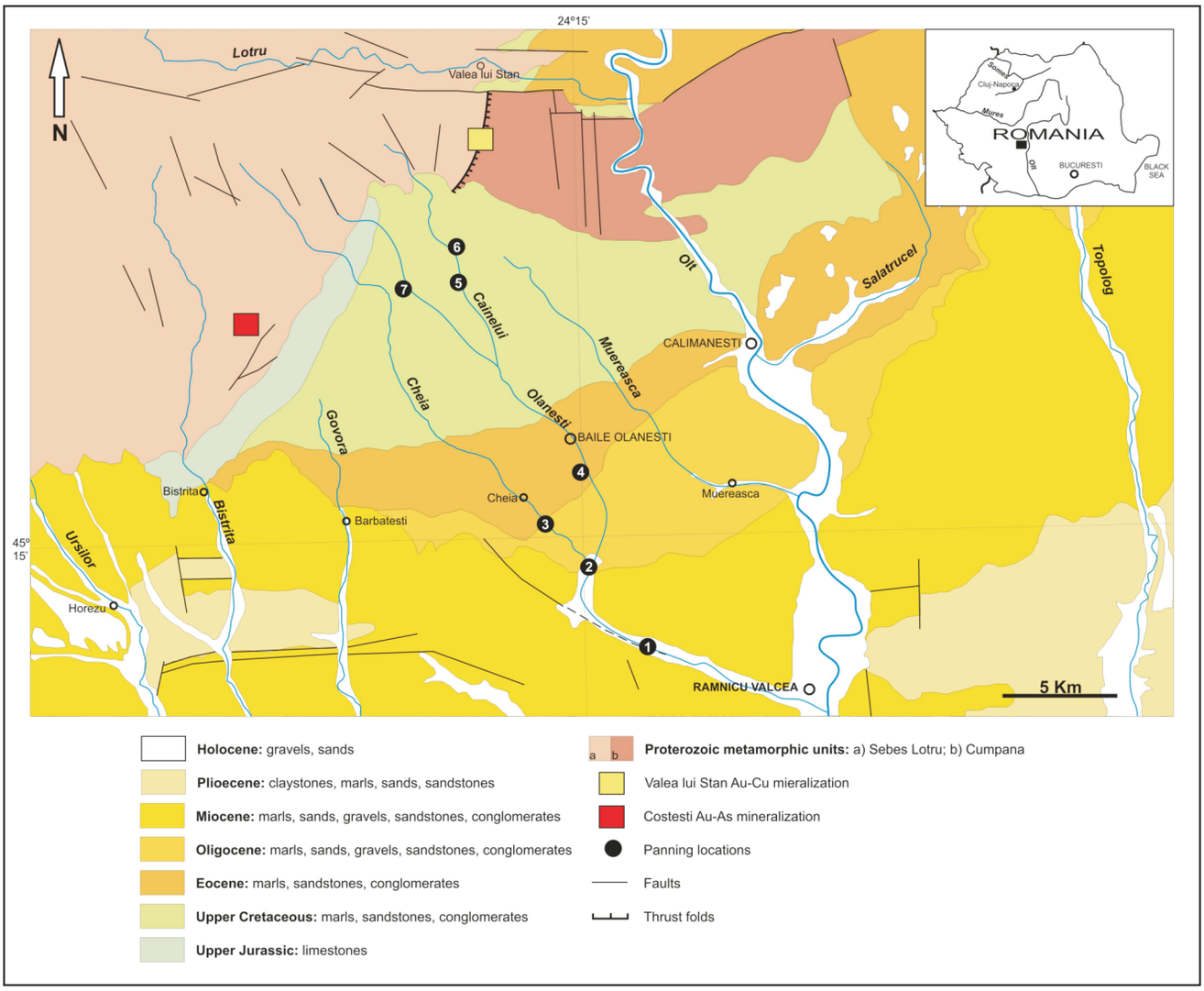

Fig. 1. Simplified geological map of the study area (modified after Murgeanu et al., 1968)

the western part of the area, Upper Cretaceous detrital deposits in the centre, and Eocene, Oligocene and Miocene detrital deposits and Holocene alluvial and colluvial deposits in the southern part (Fig. 1).

The Buila-Vânturariţa Massif is the only calcareous massif in the Căpăţânii Mountains. It consists of a NE–SW-oriented ridge (Pleş et al., 2013), mainly composed of Upper Jurassic reef carbonates (Oxfordian to Tithonian) overlying detrital silty and siliceous Middle Jurassic rocks (Dragastan, 2010).

The Upper Cretaceous sedimentary deposits are mainly formed of sandstones and conglomerates located in the eastern and northeastern part of the limestone massif (Pleş et al., 2013), with the Brezoi Formation (Campanian-Maastrichtian) as the most important sedimentary unit (Boldor et al., 1970; Todiriţă-Mihăilescu, 1973).

The Eocene, Oligocene and Miocene sedimentary deposits (Lupu et al., 1978) comprise marls, conglomerates, sandstones, sands and gravels. The most important units in the Cenozoic deposits are the Călimăneşti conglomerates (Lutetian-Ypressian), the Olăneşti marls (Priabonian-Lutetian) and the Cheia conglomerates (Oligocene). The age of the sedimentary rocks in the study area increases progressively from south to north. Overall, the sedimentary sequences have a general dip of ~45° to the south.

The Holocene deposits are represented by recent sediments, mainly gravels and sands deposited along the rivers (alluvial deposits) or boulders accumulated below the slopes (colluvial deposits).

Two localities with shear-zone-related Au-mineralization are known in the vicinity of the study area: the Valea lui Stan Cu-Au deposit (Udubaşa and Hann, 1988) in the north and the Costşti Valley As-Au deposit (Apostoloiu et al., 1990) in the west (Fig. 1).

The Au mineralization of the Valea lui Stan deposit was discovered in 1907 and was mined until 1950 (Preotesiu et al., 1973). The ore bodies consist of quartz lenses hosted by metamorphic rocks, especially on the left slope of the Valea lui Stan Valley (Udubaşa and Hann, 1988). The sulphide mineral participation is ~3–5% of the total quartz lens volume and the ore mineral assemblage consists (in order of abundance) of pyrite, arsenopyrite, chalcopyrite, marcasite, sphalerite, galena, magnetite and sporadically pyrrhotite included in arsenopyrite. The gold is included in arsenopyrite and/or chalcopyrite (Borcoş et al., 1984; Udubaşa and Hann, 1988). Traces of old mining can

be found at the junction between the Valea lui Stan Valley and Vulturul Creek (Udubaşa and Hann, 1988).

The ore bodies of the Costeşti Valley deposit are genetically related to shear zones in the Căpăţânii Mountains and are situated ~12 km south-west of the Valea lui Stan ore deposit (Apostoloiu et al., 1990). According to these authors, the ore occurrences are located especially on the Netedu Creek and on the left slope of the Costeşti Valley up Comarnici Creek. The host rocks of the Au mineralization consist of paragneisses and amphibolites and the most important ore body mined in the past was located in Netedu Creek. It was a milky white quartz lode measuring 150 m in length and 0.30 m in width. The lode contained ~10–15% sulfides and 85–90% quartz, chlorite, plagioclase, and carbonate. The ore mineral assemblage (in order of abundance) was arsenopyrite, pyrite, chalcopyrite, bismuth, bismuthinite, pyrrhotite, marcasite, sphalerite, tetrahedrite, native gold, native silver, and secondary minerals (covellite). The native gold was fine grained (5–40 μm) associated with chalcopyrite, arsenopyrite, quartz and carbonates (Apostoloiu et al., 1990).

SAMPLES AND METHODS

Fieldwork was carried out along the Cheia and Olăneşti rivers (Appendix 1) and was focused at 7 locations. From a total of 26 gold grains (Fig. 2), 24 were collected from location #3, while single gold grains from two locations #5 and #7. The largest 3 gold grains, labeled OL01-G1, OL01-G2, and OL01-G4 were found in the field by the naked eye and picked from the placer deposits of locations #3, #7, and #5, respectively. The rest of the gold grains were separated in the laboratory, using a *ZEISS Stemi 2000-C* binocular microscope, from the pan concentrate gathered in the field from location #3.

Two epoxy-cemented polished sections labeled OL01 and OL02 were manufactured using the largest 13 gold grains. Ore microscopy study of the polished sections was carried out using a *NIKON Eclipse E200* polarizing microscope. Microphotographs of the gold grains in plane-polarized and cross-polarized light were acquired using a *NIKON DS-FI3-NISD* (NIS Elements) digital camera.

Quantitative chemical analyses (WDS analytical method) were carried out using three CAMECA devices. Two datasets were acquired at the UMS 3623 – *Centre de MicroCaractérisation Raimond Castaing*, Toulouse University, France, i.e., dataset #1 and #2 using *CAMECA SXfive* and *CAMECA SXfiveFE* instruments, respectively. The datasets #3 and #4 were acquired at the Department of Geology, Babeş-Bolyai University, Romania using a *CAMECA SXfive* device.

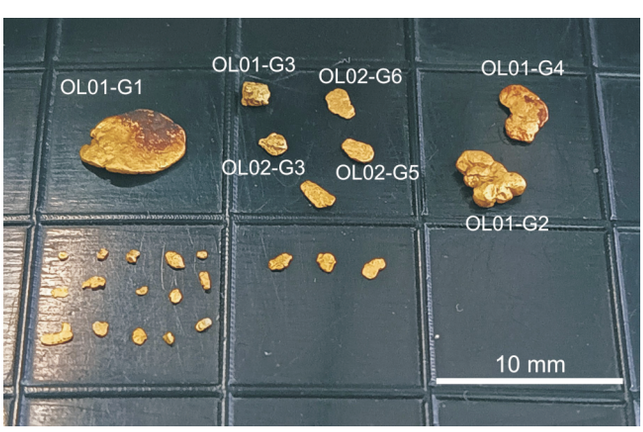

Fig. 2. The 26 gold grains were recovered from the Olăneşti and Cheia rivers

The first dataset contains results on the following elements: Ag, As, Au, Bi, Cd, Cu, Fe, Mo, Ni, Pb, S, Sb, Se and Te, while the other three regarded only Au, Ag and Cu. However, the content of all the chemical elements analysed except Au and Ag was below the detection limit. The technical conditions of the EPMA analysis are shown in Table 1 and the mean values of the detection limits/gold grain are in Table 2.

All the concentrates obtained in the field were mixed after the recovery of the gold grains and screened in 6 grain size categories for an overall microscopy study and X-ray diffraction. The screening categories were 0.063, 0.125, 0.250, 0.500, 1 and 2 mm. Each fraction was subsequently split by magnetic separation, which allowed the separation of the magnetic from the nonmagnetic minerals. Subsequently, the garnets were separated using a binocular microscope.

X-ray powder diffractions were made on several grain-size categories, from 0.063 to 0.125 mm, as well as on the magnetic concentrate with the size ranging from 0.5 to 1 mm and on the nonmagnetic fraction ranging from 0.5 to 1 mm. Additionally, X-ray diffraction analysis was carried out on garnet crystals. X-ray powder diffractions were obtained using a Bruker D8 Advance instrument at the Department of Geology, University Babeş-Bolyai, Cluj-Napoca (Romania), with Cu Kα radiation (k = 1.5418 Å), a Fe 0.01 mm filter and a *LynxEye* one-dimensional detector.

Table 1

The analytical conditions used to acquire the four EPMA datasets

Dataset #1				
Element	Energy line	Standard	kV	nA
Au	Ma	Au	15	20
Cu	Ka	chalcopyrite	15	20
Ag	La	Ag	15	20
As	La	arsenopyrite	15	20
Co	Ka	Co	15	20
Ni	Ka	Ni	15	20
Se	La	Se	15	20
Mo	La	Mo	15	20
Te	La	HgTe	15	20
Bi	Ma	Bi	15	20
Cd	La	Cd	15	20
S	Ka	chalcopyrite	15	20
Pb	Ma	PbS	15	20
Sb	La	SbS	15	20
Fe	Ka	chalcopyrite	15	20
Zn	Ka	ZnS	15	20
Dataset #2				
Au	Ma	Au	15	20
Cu	Ka	chalcopyrite	15	20
Ag	La	Ag	15	20
Dataset #3 and Dataset #4				
Au	Ma	Au	15	10
Cu	Ka	Cu	15	10
Ag	La	AgBr	15	10

Table 2

Mean values of the detection limits/gold grain in wt.% and the number of point analyses

Dataset	Gold grain	Au	Ag	Cu	As	Bi	Cd	Co	Fe	Mo	Ni	Pb	S	Se	Sb	Te	Zn	No. of points
1	OL01-G1	0.37	0.13	0.16	0.09	0.28	0.11	0.13	0.12	0.10	0.12		0.08	0.09	0.10	0.21		6
4	OL01-G1	0.78	0.26	0.31														7
1	OLO1-G2	0.37	0.13	0.16	0.08	0.28	0.11	0.14	0.12	0.11	0.12		0.08	0.09	0.10	0.22		7
2	OLO1-G2	0.32	0.19	0.16														5
3	OLO1-G2	0.77	0.26	0.31														10
1	OLO1-G3	0.35	0.13	0.16	0.09	0.27	0.12	0.13	0.11	0.11	0.12		0.08	0.09	0.09			5
4	OLO1-G4	0.77	0.27	0.31														8
1	OL02-G1	0.37	0.12	0.16		0.28	0.11	0.13	0.11	0.11	0.12	0.57	0.07	0.09	0.09	0.19		5
2	OL02-G1	0.42	0.19	0.16														3
3	OL02-G1	0.68	0.22	0.27														12
1	OL02-G2	0.34	0.12	0.16	0.08	0.28	0.11	0.13	0.11	0.10	0.11	0.49	0.09	0.09	0.09	0.20	0.19	10
3	OL02-G2	0.65	0.23	0.27														11
1	OL02-G3	0.35	0.13	0.16	0.08	0.26	0.12	0.13	0.12		0.12		0.07		0.09			3
3	OL02-G3	0.65	0.24	0.27														11
1	OL02-G4	0.35	0.13	0.16	0.09	0.26	0.11		0.12	0.11	0.12		0.07	0.09	0.09	0.21		3
2	OL02-G4	0.39	0.20	0.16														5
3	OL02-G4	0.66	0.24	0.27														12
1	OL02-G5	0.36	0.13	0.16	0.08	0.28	0.11	0.14	0.12	0.11	0.12		0.08	0.09		0.21		3
2	OL02-G5	0.40	0.20	0.16														4
3	OL02-G5	0.64	0.24	0.27														8
2	OL02-G6	0.41	0.19	0.16														7
3	OL02-G6	0.65	0.22	0.27														12
2	OL02-G7	0.41	0.19	0.16														7
3	OL02-G7	0.66	0.22	0.27														7
Total number of point analyses:																		171

RESULTS

X-RAY DIFFRACTION

The XRD results indicate that the 0.063 to 0.125 mm grain-size concentrate is composed of quartz, magnetite, ilmenite, microcline, albite, apatite, zoisite, epidote, almandine and pyrite. The 0.5 to 1 mm nonmagnetic grain-size concentrate is composed of quartz, albite, almandine and pyrite. The 0.5 to 1 mm grain-size magnetic concentrate is composed of magnetite and almandine, and the garnet concentrate is dominated by almandine, with minor amounts of muscovite and quartz.

NATIVE GOLD GRAIN MORPHOLOGICAL ANALYSIS

The morphological classification of the native gold grains (Fig. 3) was made according to Barrios et al. (2015), who separated the gold grains by taking into account their sphericity (discoidal, subdiscoidal, spheroidal, and elongated shape) and roundness (rounded, intermediate, and angular) appearance.

The OL01 polished section comprised 4 gold grains numbered from OL01-G1 to OL01-G4. The OL01-G1 gold grain (Fig. 3A, D) has a discoidal rounded shape and is partly covered by a black crust, which presumably indicates a close contact of the gold grain with sulfides that have oxidized. The OL01-G2 (Fig. 3B, E) gold grain is subdiscoidal rounded to intermediate with an attached quartz crystal. The OL01-G4 (Fig. 3C, F) subdiscoidal-rounded gold grain is heart-shaped, and is accompanied by quartz. The morphology of these gold grains together with the related quartz crystals indicate short-distance transport from the source.

The OL02 polished section comprises smaller gold grains with spheroidal and elongated shapes with intermediate to rounded edges (Fig. 3G, L). These gold grains were recovered from the heavy mineral concentrate from location #3.

ORE MICROSCOPY

Polished sections with the alluvial gold grains were studied using a polarizing microscope in plane-polarized and crossed-polarized reflected light. The colour of the gold grains is intense yellow (high reflectance) and they rarely host inclusions of other minerals, e.g. pyrite, quartz (Fig. 4), and galena (Fig. 5A, B). The ore microscopy observations did not revealed any colour zoning, nor rims with a different reflection colour, nor variations in the anomalous anisotropy of the gold grains (Fig. 4).

GEOCHEMICAL ANALYSES

Quantitative chemical analyses were carried out on 11 gold grains giving a total of 171 analytical points acquired on 3 different EPMA instruments and organized in four datasets. The first dataset consists of 42 data points, the second one 31 points,

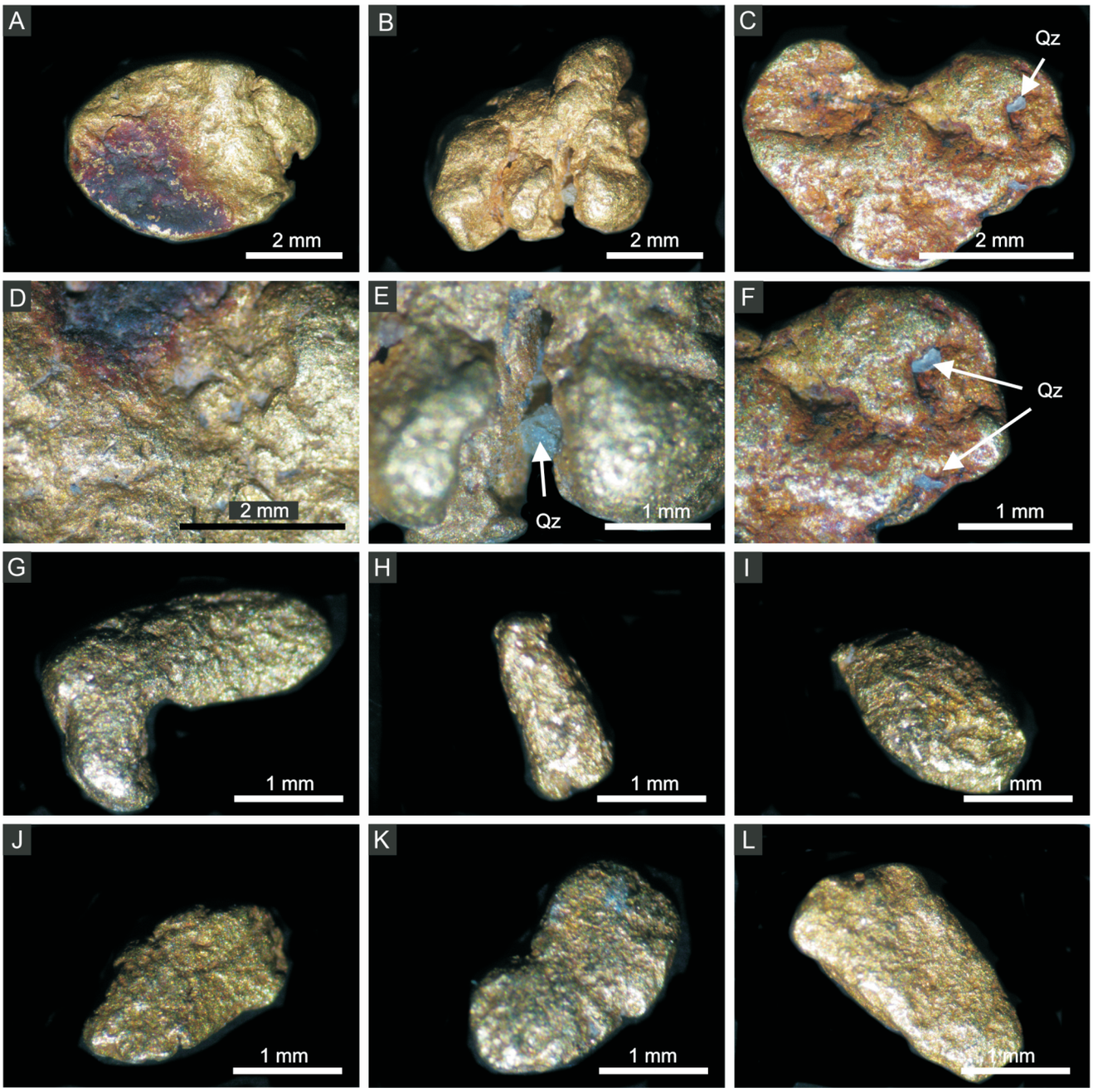

Fig. 3. Binocular microscope images of different gold grains from the study area

A – OL01-G1 – discoidal gold grain with black reddish oxidation crust, indicating an influence of related sulphides (pyrite/base metal sulphides?); **B** – OL01-G2 – subdiscoidal gold grain with associated quartz grains; **C** – OL01-G4 – subdiscoidal gold grain with quartz grains preserved within the cavities of the gold grain; **D** – detail of the OL01-G1 gold grain showing its irregular surface and the thin oxidation crust; **E** – detail of OL01-G2 revealing the preserved quartz grain located in a "shadow" zone, protected by two globular gold protuberances; **F** – detailed image of OL01-G4, showing the thin reddish oxidation crust that partly covers the gold grain and the quartz preserved within the pits of the particle; **G–L** – selection of small gold particles with elongated shapes and intermediate to rounded edges/borders

the third one 73 points, and the fourth dataset 25. A total of 132 points out of 171 are valid, with the total (in wt.%) in the range 98–102. The analytical point locations are shown in Figures 5 and 6 on the microphotographs of the gold grains in reflected light and Table 3 summarizes the whole EPMA points/gold grain/dataset.

The OL01-G2 gold grain (Table 3, dataset #1) is the most heterogeneous one, with a five-point analysis indicating a rather constant Ag content ranging from 13.71 to 14.04 wt.% and another 2-point analysis revealing a significantly lower Ag content, ranging from 2.00 to 2.80 wt.%. The other gold grains have homogeneous chemical compositions.

The maximum Ag content of a gold grain was 20.77 wt.%, detected within grain OL02-G4, dataset #2, while the minimum Ag content is 2.00 wt.%, measured within grain OL01-G2, dataset #1.

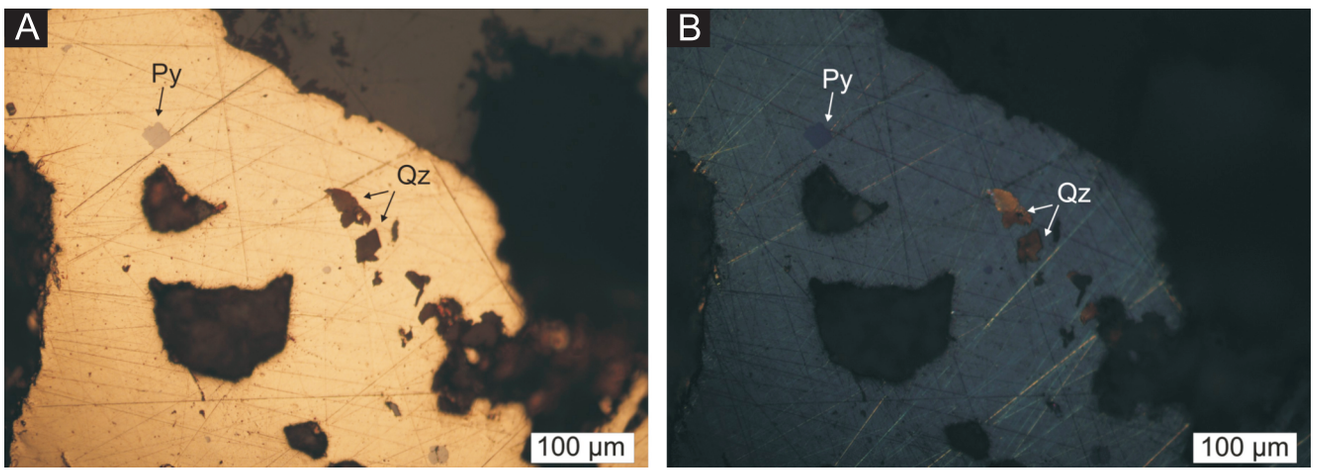

Fig. 4. Microphotographs in plane-polarized light (A) and in cross-polarized light (B) of the OL02-G3 gold grain, with pyrite (Py) and quartz (Qz) inclusions; note the anomalous anisotropy of the gold

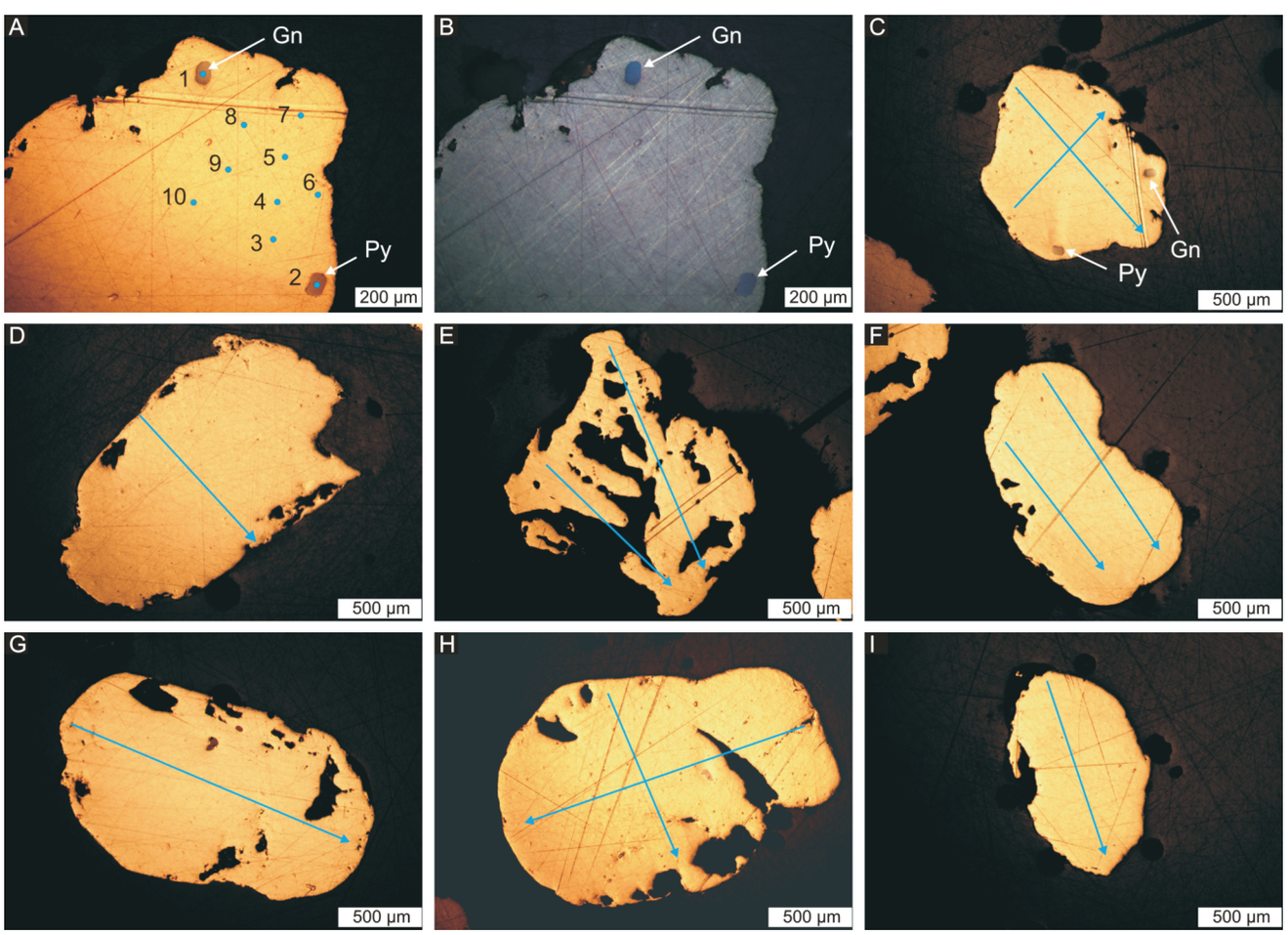

Fig. 5. Microphotographs (A, C–I in plane-polarized light; and B in cross-polarized light) of gold grains with the point analysis dataset #1 (Table 3) indicated by blue dots, and the orientation of the point analysis dataset #3 indicated by blue arrows; the gold grain labels are OLO2-G1 (D), OL02-G2 (A, B, C), OL02-G3 (E), OL02-G4 (F), OL02-G5 (G), OL02-G6 (H), and, OL02-G7 (I); the gold grain OL02-G2 (A, B) hosts galena (Gn) and pyrite (Py) inclusions

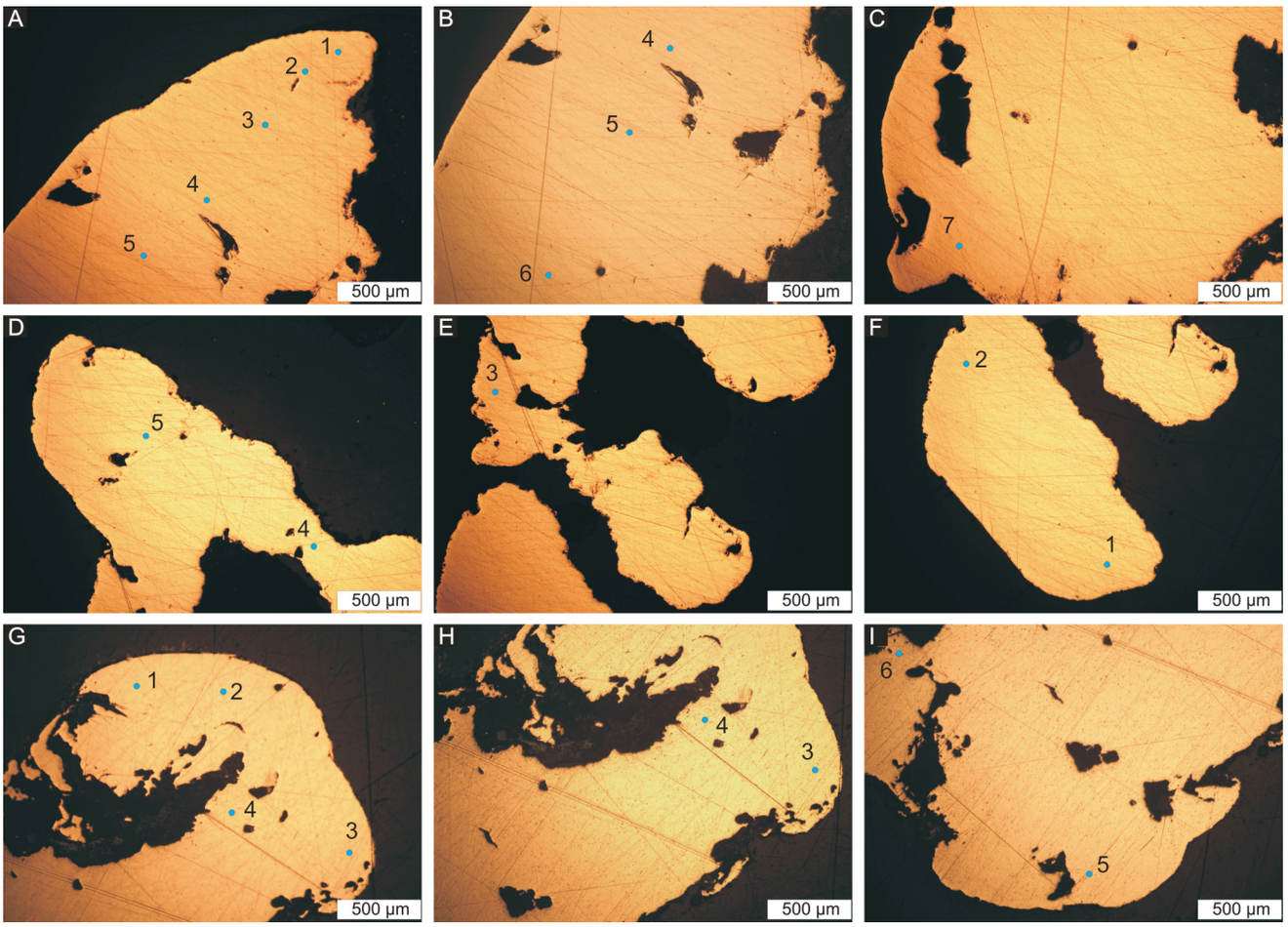

Fig. 6. Microphotographs in plane-polarized light of the OL01-G1 (A, B, C), OL01-G2 (D, E, F) and OL01-G4 (G, H, I) gold grains with the analytical points dataset #4 indicated by blue dots

Apart the gold grains, pyrite and galena inclusions within the OL020-G2 gold grain were also analyzed (Fig. 5A) and the EPMA results corroborated the ore microscopy observation.

DISCUSSION

Youngson and Craw (1999) separated gold placers into i) primitive placers or first-cycle placers formed within high-gradient rivers, where the water flows on or near bedrock, and ii) trunk placers developed within low-gradient rivers with a bed load of gravel and usually occurring downstream of the primitive placers, being multicycle or multisource deposits. According to this classification, the placer deposits in panning locations #1 and #2 are trunk placers, at locations #5, #6, and #7 they are primitive placers, while at panning location #3, there is an intermediate placer style sharing characteristics of both trunk and primitive placers, which likely seems to correspond to the transition zone as indicated by Youngson and Craw (1999).

According to the visual morphological classification diagram of Barrios et al. (2015), the larger gold particles, with sizes ranging from 3 to 6 mm, have subdiscoidal shapes and rounded surfaces, while the smaller gold particles, with sizes ranging from 1 to 2 mm have elongated shapes, and the roundness is variable from intermediate to rounded.

The OL01-G2 and OL01-G4 gold grains were collected from primitive placers in the northern part of the study area towards the waterfront of the Câinelui and Olăneşti rivers and show predominantly subdiscoidal shapes (e.g., OL01-G4 is subdiscoidal, and OL01-G2 is subdiscoidal to spheroidal). Both these gold grains are still associated with the quartz gangue of the primary ore. OL01-G1, which was collected from the transition zone between primitive and trunk placers along the Cheia River in the southern part of the study area, has a discoidal shape and is free of primary gangue minerals.

The mineral concentrates containing also native gold grains consist of garnets (almandine), quartz, plagioclase feldspars (albite), potassic feldspars (microcline), micas (muscovite), magnetite, ilmenite, apatite, epidotes (zoisite) and pyrite.

The ore microscopy study revealed no reflectance colour variation within the gold grains or on their borders suggesting the chemical homogeneity of the gold grains, which was also corroborated by the EPMA results. The ore microscopy study revealed the presence of pyrite and galena inclusions within the gold grains (OL02-G2 and OL02-G3). The presence of such sulphide inclusions hosted by placer gold grains indicates the preservation of the primary/original chemical composition of the gold because sulfides unprotected by a gold cover are rapidly altered or removed in the placer environment (Desborough, 1970).

Table 3

EPMA results on the gold grains in the Olăneşti area

Dataset #1				OL02-G2				OL02-G4				Dataset #3				7	18.70	80.15	98.85	OL02-G7			
OL01-G1				no.	Ag	Au	Total	no.	Ag	Au	Total	OL02-G1				9	18.40	81.09	99.49	no.	Ag	Au	Total
no.	Ag	Au	Total	1	11.64	88.82	100.46	1	19.53	78.84	98.37	no.	Ag	Au	Total	10	18.28	82.03	100.31	1	9.25	90.50	99.75
1	11.84	88.55	100.39	2	11.87	88.47	100.34	2	20.77	79.88	100.65	2	6.47	92.21	98.67	11	17.96	82.28	100.24	2	7.65	90.38	98.02
2	11.78	89.80	101.58	3	11.71	88.66	100.37	3	20.44	81.18	101.62	3	6.81	92.52	99.33	OL02-G4				3	9.26	90.85	100.12
3	11.91	88.78	100.69	4	11.85	89.35	101.20	4	20.48	80.94	101.42	4	6.22	94.43	100.65	no.	Ag	Au	Total	4	8.85	89.65	98.50
4	11.96	89.04	101.00	5	11.81	88.84	100.65	5	20.44	80.25	100.69	5	6.50	93.45	99.94	1	14.94	84.30	99.24	6	9.37	89.98	99.35
5	12.40	89.38	101.78	6	11.57	88.77	100.34	OL02-G5				6	6.31	93.51	99.82	3	15.16	84.25	99.42	dataset #4			
OL01-G2				7	11.50	89.17	100.67	no.	Ag	Au	Total	7	6.47	94.32	100.79	4	15.12	84.86	99.97	OL01-G1			
no.	Ag	Au	Total	OL02-G3				1	11.74	87.83	99.57	8	6.96	92.58	99.55	5	15.25	84.31	99.57	no.	Ag	Au	Total
1	2.80	95.91	98.71	no.	Ag	Au	Total	2	12.80	88.09	100.89	9	6.82	93.37	100.19	6	15.50	84.24	99.74	3	11.20	87.79	98.98
2	2.00	99.30	101.30	1	19.76	81.53	101.29	3	12.55	88.69	101.24	10	3.10	96.03	99.13	7	15.43	84.91	100.34	5	11.19	88.59	99.78
3	13.91	86.25	100.16	2	19.62	80.46	100.08	4	12.05	88.16	100.21	12	6.06	92.05	98.11	9	14.66	86.82	101.48	6	10.99	87.56	98.55
4	14.04	86.74	100.78	3	20.23	80.67	100.90	OL02-G6				OL02-G2				11	15.18	84.33	99.51	7	11.27	90.27	101.54
5	14.01	86.91	100.92	OL02-G4				no.	Ag	Au	Total	no.	Ag	Au	Total	OL02-G5				OL01-G2			
6	13.71	86.11	99.82	no.	Ag	Au	Total	1	11.99	88.63	100.62	1	10.68	87.59	98.27	no.	Ag	Au	Total	no.	Ag	Au	Total
7	14.04	85.72	99.76	1	20.73	79.42	100.15	2	9.88	91.99	101.87	2	10.26	88.15	98.41	1	18.16	79.87	98.03	1	12.51	87.02	99.53
OL01-G3				2	20.65	78.98	99.63	3	12.21	89.61	101.82	3	10.13	89.06	99.19	2	18.04	80.30	98.33	3	12.58	86.81	99.39
no.	Ag	Au	Total	OL02-G5				4	12.02	88.45	100.47	4	10.67	89.06	99.72	4	18.50	80.88	99.38	6	12.63	87.01	99.63
1	19.91	80.78	100.69	no.	Ag	Au	Total	5	12.68	88.27	100.95	5	10.26	89.18	99.44	5	18.85	80.28	99.14	8	12.03	87.36	99.39
2	19.50	78.74	98.24	1	10.14	89.96	100.10	6	10.33	89.85	100.18	6	10.35	88.79	99.14	8	19.15	79.13	98.28	9	12.68	85.66	98.34
3	19.34	80.95	100.29	2	11.76	87.13	98.89	7	12.16	88.57	100.73	8	10.50	88.09	98.59	OL02-G6				OL01-G4			
4	20.29	80.84	101.13	3	12.31	87.57	99.88	OL02-G7				9	10.51	87.55	98.05	no.	Ag	Au	Total	no.	Ag	Au	Total
5	19.80	79.99	99.79	dataset #2				no.	Ag	Au	Total	10	18.66	80.44	99.10	1	8.40	90.44	98.84	3	13.04	85.88	98.92
OL02-G1				OLO1-G2				1	8.52	90.43	98.95	11	16.66	83.04	99.70	3	10.86	87.43	98.29	4	12.86	86.35	99.21
no.	Ag	Au	Total	no.	Ag	Au	Total	2	11.25	89.30	100.55	OL02-G3				5	7.63	92.90	100.54	5	13.44	85.27	98.71
1	6.96	94.56	101.5	1	13.59	85.24	98.83	3	12.10	89.57	101.67	no.	Ag	Au	Total	6	11.32	86.75	98.07				
2	6.70	91.56	98.26	OL02-G1				4	9.75	91.82	101.57	1	17.45	81.11	98.56	7	11.19	88.10	99.29				
3	7.18	92.15	99.33	no.	Ag	Au	Total	5	12.05	88.56	100.61	2	17.96	81.18	99.14	9	9.96	89.75	99.71				
4	7.03	93.36	100.39	1	10.14	91.81	101.95	6	10.65	88.14	98.79	4	18.66	80.11	98.77	10	11.37	87.68	99.05				
				2	7.70	94.16	101.86	7	11.61	88.37	99.98	5	17.84	80.28	98.11	11	8.82	91.52	100.34				
				3	8.57	93.41	101.98					6	18.67	81.55	100.22	12	10.98	87.48	98.46				

The EPMA results on the alluvial gold grains reveal their mixed Au-Ag composition with Ag ranging from 7.31 to 19.77 wt.% and Au ranging from 80.26 to 93.16 wt.% (Table 4). The microchemical analyses of the gold grains suggest a generally continuous chemical composition variation instead of distinct populations. The chemical formula for each gold grain calculated based on the mean wt.% values is shown in Table 4 and the mean values of Au and Ag (in wt.%) for each gold grain are plotted in Figure 7.

Table 4

The mean values of Au and Ag (in wt.%) for each gold grain sorted in ascending order of Au content, the calculated chemical formulae, and the panning locations

Gold grain	Au [wt.%]	Ag [wt.%]	Total [wt.%]	Calculated chemical formula	Panning location
OL01-G3	80.26	19.77	100.03	$Au_{0.69}Ag_{0.31}$	#3
OL02-G3	80.99	19.04	100.03	$Au_{0.70}Ag_{0.30}$	#3
OL02-G4	81.39	18.73	100.12	$Au_{0.70}Ag_{0.30}$	#3
OL02-G5	85.50	14.08	99.58	$Au_{0.77}Ag_{0.23}$	#3
OL01-G4	85.83	13.11	98.94	$Au_{0.78}Ag_{0.22}$	#5
OL01-G2	87.19	12.24	99.43	$Au_{0.80}Ag_{0.20}$	#7
OL02-G2	87.98	11.79	99.77	$Au_{0.80}Ag_{0.20}$	#3
OL01-G1	88.83	11.57	100.40	$Au_{0.81}Ag_{0.19}$	#3
OL02-G6	89.23	10.83	100.06	$Au_{0.82}Ag_{0.18}$	#3
OL02-G7	89.86	9.86	99.72	$Au_{0.83}Ag_{0.17}$	#3
OL02-G1	93.16	7.31	100.47	$Au_{0.87}Ag_{0.13}$	#3

The chemical composition of the alluvial gold from the study area is presumed to reflect the chemical composition of the primary gold from the orogenic gold mineralization known upstream farther north and west, based on the preservation of sulphide inclusions in the alluvial gold grains. The identified chemical compositions of the presumed orogenic gold from the Olăneşti River placers are within the range of orogenic gold known elsewhere in the world, e.g., the Hog Mountain, Southern Appalachians, US, with Au contents ranging between 89.7 and 91.4 wt.%, and Ag contents ranging between 8.31 and 9.10 wt.% (Brueckner et al., 2021), or the Northern Cariboo Gold District, British Columbia, Canada, with the Ag contents in the orogenic gold usually ranging from 5 to 20 wt.% (Chapman and Mortensen, 2016).

The gold grain labeled OL01-G2 shows the most heterogeneous chemical composition, with a two-point analysis (dataset #1) indicating the lowest Ag contents, i.e., 2.00 and 2.80 wt.%, and a five-point analysis ranging from 13.71 to 14.04 wt.% Ag. In these results, the different chemical compositions were determined for the outer part and the inner part of the gold grain, respectively. Accordingly, the BSE image (Fig. 8) reveals a whitish rim around the OL01-G2 gold grain, which suggests the presence of a thin gold-rich/silver-poor external layer. Such gold-enriched rims certainly occur, though their mechanism of formation has long been debated. One means of producing an Au-enriched rim is by depletion in silver of the gold grain. This mechanism was proposed, for instance, by Desborough (1970), through selective depletion in Ag by aqueous solutions, by Krupp and Weisser (1992) by Ag removal due to the presence of chloride in the waters, and by Knight et al. (1999a) by leaching of Ag (Cu) and the formation of a porous gold-enriched rim.

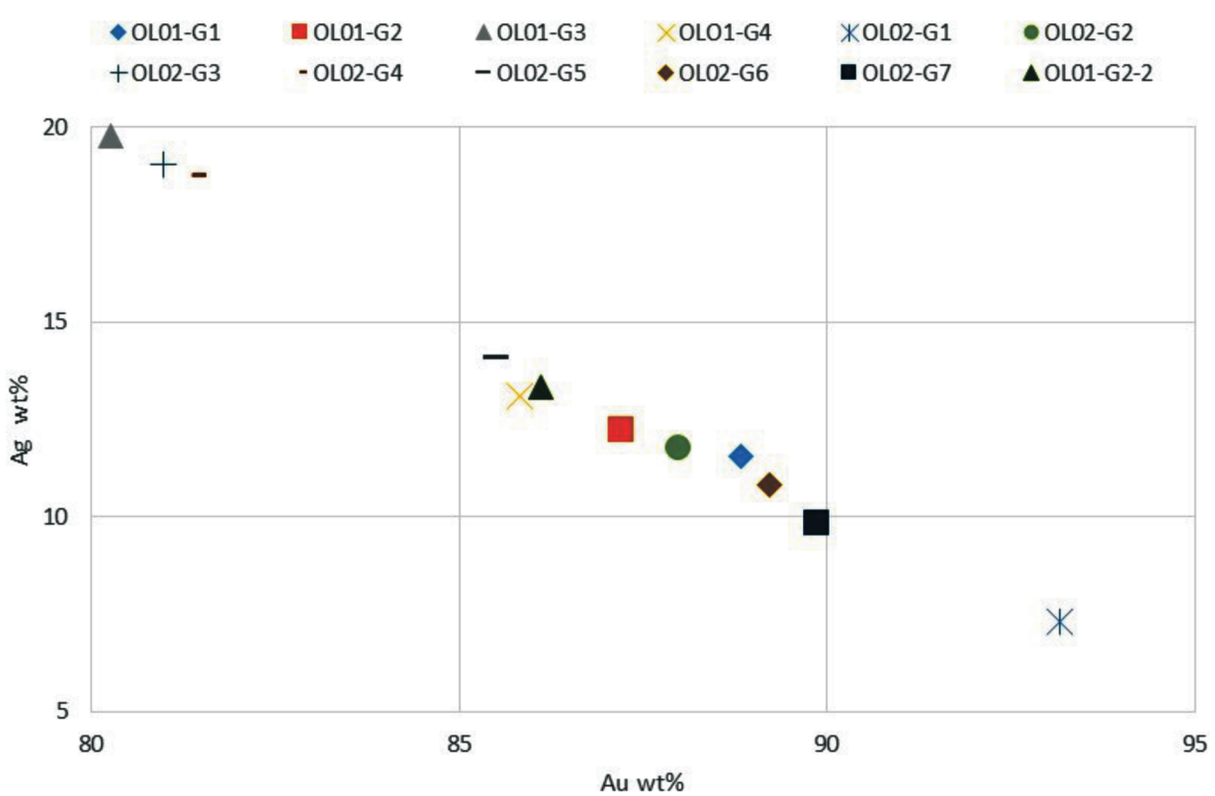

Fig. 7. Plot of the Au and Ag content (mean values in wt.%) of the gold grains recovered from the Olăneşti and Cheia rivers

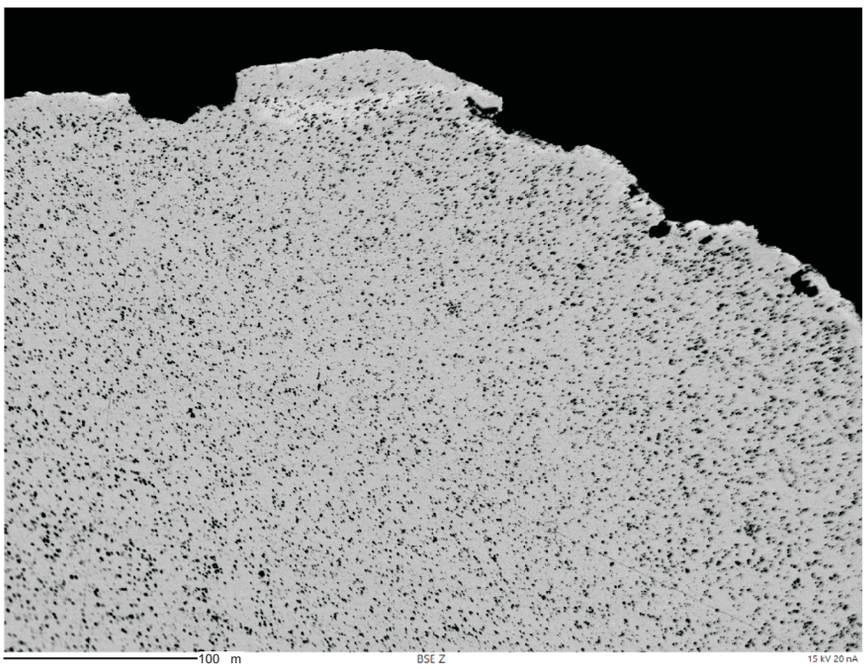

Fig. 8. BSE image of the OL01-G2 gold grain showing the Ag-rich rim (whitish) and the homogeneous chemical composition of the interior of the grain as suggested by the uniform grey tint

Alternatively, Groen et al. (1990) considered that a combination of self-electrorefining of native gold grains and cementation is responsible for the formation of a gold-rich rim developed on native gold grains, while selective leaching of silver from the outer zone of the grains perhaps combined with diffusion of Ag from the inner part of native gold grains was not considered by Groen et al. (1990) as an effective process to form such supergene gold enrichment rims. Two gold-enrichment rim formation mechanisms were considered by Youngson and Craw (1999) to contribute, via silver dissolution and precipitation of authigenic gold, to produce this particular feature that helps discriminate between primary gold and placer gold grains. Similar views were expressed by Wierchowiec et al. (2021) who considered that the leaching of Ag together with the precipitation of authigenic gold (by several processes) creates the gold-enriched/silver-depleted rims of placer gold grains.

Groen et al. (1990) suggested that the rims are thicker on native gold grains that were transported across longer distances and consequently show flake-type morphology, and are thinner or absent on the gold grains that experienced shorter transport. In our case, the gold grain OL01-G2 was found in the upper part of the Olăneşti River at ~6 km from the presumed gold source (Fig. 1) in a primary placer, which implies short-distance transport. On the other hand, Knight et al. (1999a) considered that the formation of the gold-enriched rim takes place in buried sediments, while the rims are removed by abrasion in actively transported sediments. Additionally, almost all the placer gold grains examined by Knight et al. (1999b) from Klondike District, Yukon Territory, Canada have at least a partial gold-enriched rim, while the lode gold shows no rims. Other gold grains from the Olăneşti area seem to have gold-enriched rims because several point analyses showing significantly lower Ag grades close to the borders were obtained, though these results are compromised because the total of their analyses exceeds the confidence interval, i.e., 102.23 and 97.73 wt.%, respectively. Additionally, these rims were not observed by means of ore microscopy, probably due to their small width. All in all, the scarce presence of gold-enriched rims may be the result of short-distance of transport of the gold grains and the relatively brief time of processing of the grains since their removal from the original orogenic gold ore bodies. The OL01-G2 grain that certainly has a gold-rich rim probably spent more time buried in sediments so that a rim developed. However, the proportion of such grains is small, and this fact allow us to conclude that erosion of the primary gold source (orogenic Au lodes) is currently in progress and that most of the gold grains are being actively processed.

The presence of related ore or/and gangue minerals from the primary ore minerals association, which are still attached to the gold grains within the placer deposits, is considered to be another indicator of short-distance transport of the native gold grains. For example, the OL01-G2 and OL01-G4 gold grains still have quartz remains attached to the gold surface, and this relationship indicates a very short distance from the primary gold source. This observation is in agreement with the geographic position of the panning locations #7 and #5 that yielded the two gold grains, situated towards the headwater of the Cainelui drainage basin, close to the presumed primary gold sources, e.g., the Valea lui Stan deposit.

CONCLUSIONS

Twenty-six gold particles weighing ~0.5 g were collected from 3 panning locations in the Olăneşti area along several watercourses, i.e., the Olăneşti River, Cheia River, Câinelui River, Olăneşti tributary creek and Câinelui tributary creek. The gold placers identified belong to the primitive, intermediate/transition zone, and are of trunk placer type.

Most of the native gold grains, which may reach up to 6 mm in size, were found between the river deposits and the bedrock.

The largest gold grains have discoidal to subdiscoidal shapes; their roundness ranges from rounded to sub-rounded, with locally preserved remnants of the primary quartz gangue on their surface. The small gold particles show elongated shapes, an intermediate to rounded appearance, with no associated quartz preserved.

The EPMA quantitative analyses carried out on 11 gold grains revealed a generally continuous variation of the gold and silver content with Ag ranging from 7.31 to 19.77 wt.% and Au ranging from 80.26 to 93.16 wt.%. A thin Au-rich rim, with <3 wt.% Ag was observed on a single gold grain. The primary gold source is inferred to be orogenic gold mineralization from the Sebeş-Lotru metamorphic unit, which also hosts the Valea lui Stan and Costeşti Au-bearing ore deposits.

Acknowledgements. Many thanks are addressed to P. de Parseval and S. Guy (UMS 3623 – Centre de MicroCaractérisation Raimond Castaing, Toulouse University, France) for their support during EPMA analyses. The fieldwork expenses were covered by the POCU/380/6/13/123886 "Antreprenoriat pentru inovare prin cercetare doctorală şi postdoctorală" grant of Babeş-Bolyai University, Cluj-Napoca, Romania (SD).

REFERENCES

Apostoloiu, A., Berbeleac, I., Popescu, D., 1990. The As-Au quartz veins in the Costeşti Valley, Căpăţîna Mountains, South Carpathians. Révue Roumaine de Géologie, Géographie et Géologie, **34**: 25–34.

Balintoni, I., 1997. The geotectonics of the metamorphics in Romania (in Romanian). Editura Carpatica, Cluj-Napoca.

Balintoni, I., Balica, C., Ducea, M.N., Hann, H.P., Şabliovski, V., 2010. The anatomy of a Gondwanan terrane: The Neoproterozoic–Ordovician basement of the pre-Alpine Sebeş–Lotru composite terrane (South Carpathians, Romania). Gondwana Research, **17**: 561–572. https://doi.org/10.1016/j.gr.2009.08.003

Barrios, S., Merinero, R., Lozano, R., Orea, I., 2015. Morphogenesis and grain size variation of alluvial gold recovered in auriferous sediments of the Tormes Basin (Iberian Peninsula) using a simple correspondence analysis. Mineralogy and Petrology, **109**: 679–691. https://doi.org/10.1007/s00710-015-0399-x

Bedelan, H., Bedelean, A., 2001. Contributions to the study of alluvial gold from Valea Pianului area (Alba district). Studia Universitatis Babeş-Bolyai, Geologia, **46**:161–169.

Boldor, C., Stilla, A., Iavorschi, M., Dumitru, I., 1970. New data regarding the stratigraphy and tectonics of the Mesozoic sedimentary deposits from Olăneşti (Southern Carpathians) (in Romanian). Dări de Seamă Institutul Geologic, **55**: 217–221.

Borcoş, M., Kraütner, H.,G., Udubaşa, G., Săndulescu, M., Năstăsescu, S., Bițoianu, C., 1984. Geological Atlas 1:1000000, Map of the Mineral Resources – Explanatory note. Ministry of Geology, Institute of Geology and Geophysics, Bucharest.

Brueckner, S.M., Kline, A.K., Bilenker, L.D., Poole, J., Whitney, M.S., 2021. Mineral chemistry and sulfur isotope geochemistry from tonalite-hosted, gold-bearing quartz veins at Hog Mountain, Southwestern Appalachians: implications for gold precipitation mechanism, sulfur source, and genesis. Economic Geology, **116**: 357–388. https://doi.org/10.5382/econgeo.4786

Cauuet, B., Bedelean, A., Boussicault, M., Carré, R., Ciugudean, H., Lehrberger, G., Rico, C., Ruttner, V., Tămaş, C., 1999. Mines d'or antiques de Dacie. Valée du Pianul et district de Roşia Montană (Carpates Méridionales, Roumanie). Rapport de mission archéologique, Université de Toulouse le Mirail, France.

Chapman, R.J., Mortensen, J.K., 2016. Characterization of gold mineralization in the Northern Cariboo Gold District, British Columbia, Canada, through integration of compositional studies of lode and detrital gold with historical placer production: a template for evaluation of orogenic gold districts. Economic Geology, **111**: 1321–1345. https://doi.org/10.2113/econgeo.111.6.1321

Cook, N.J., Ciobanu, C.L., 2004. Preface. in "Au-Ag-Telluride Deposits of the Golden Quadrilateral, Apuseni Mts., Romania. Guidebook of the International Field Workshop of IGCP Project 486 Alba Iulia, Romania" (eds. N. Cook and C.L. Ciobanu): 1–4. IAGOD Guidebook Series 12, International Association on the Genesis of Ore Deposits (IAGOD), Oslo.

Dragastan, O., 2010. Getic carbonate platform-stratigraphy of Jurassic and lower Cretaceous, reconstructions, paleogeography, provinces and biodiversity (in Romanian). Editura Universitatii din Bucuresti.

Desborough, G.A., 1970. Silver depletion indicated by microanalysis of gold from placer occurrences, Western United States. Economic Geology, **65**: 304–311. https://doi.org/10.2113/gsecongeo.65.3.304

Galcenco, V., Veress, E., Velciov, G., 1995. L'or alluvionnaire du cours moyen des riviéres Mureş, Strei et Crişul Alb (Roumanie). Romanian Journal of Mineralogy, **76**: 105–110.

Ghiţulescu, T.P., Socolescu, M., 1941. Etude géologique et minière des Monts Métallifères (Quadrilatère aurifère et regions environnantes). Annuaire Institut Géologique Roumain, **21**: 181–465.

Groen, J.C., Craig, J.R., Rimstidt, J.D., 1990. Gold rich rim formation on electrum grains in placers. Canadian Mineralogist, **28:** 207–228.

Iancu, V., Màruntiu, M., Johan, V., Ledru, E., 1998. High-grade metamorphic rocks in the pre-Alpine nappe stack of the Getic-Supragetic basement (Median Dacides, South Carpathians, Romania). Mineralogy and Petrology, **63:** 173–198. https://doi.org/10.1007/BF01164150

Knight, J., Morison, S., Mortensen, J., 1999a. The relationship between placer gold particle shape, rimming, and distance of fluvial transport as exemplified by gold from the Klondike District, Yukon Territory, Canada. Economic Geology, **94**: 635–648. https://doi.org/10.2113/gsecongeo.94.5.635

Knight, J., Mortensen, J., Morison, S., 1999b. Lode and placer gold composition in the Klondike District, Yukon Territory, Canada: implications for the nature and genesis of Klondike placer and lode gold deposits. Economic Geology, **94**: 649–664. https://doi.org/10.2113/gsecongeo.94.5.649

Krupp, R.E., Weiser, T., 1992. On the stability of gold-silver alloys in the weathering environment. Mineralium Deposita, **27**: 268–275. https://doi.org/10.1007/BF00193397

Lupu, M., Popescu, B., Szasz, L., Hann, H., Gheuca, I., Dumitrica, P., Popescu, GH., 1978. Geological map of Romania, 1:50.000, sheet 126a, Vânturarţta (Olăneşti) (in Romanian). Institutul Geologie şi Geofizică, Bucureşti.

Medaris, G., Ducea, M., Ghent, E., Iancu, V., 2003. Conditions and timing of high-pressure Variscan metamorphism in the South Carpathians, Romania. Lithos, **70**: 141–161. https://doi.org/10.1016/S0024-4937(03)00096-3

Murgeanu, G., Mihăilă, N., Giurgea, P., Bombiţă, G., Lupu, M., 1968. Geological map of Romania, 1:200 000, 34. Piteşti.

Neubauer, F., Lips, A., Kouzmanov, K., Lexa, J., Ivăşcanu, P., 2005. Subduction, slab detachment and mineralization: the Neogene in the Apuseni Mountains and Carpathians. Ore Geology Reviews, **27**: 13–44. https://doi.org/10.1016/j.oregeorev.2005.07.002

Pleş, G., Mircescu, C.V., Bucur, I.I., Săsăran, E., 2013. Encrusting micro-organisms and microbial structures in Upper Jurassic limestones from the Southern Carpathians (Romania). Facies, **59**: 19–48. https://doi.org/10.1007/s10347-012-0325-1

Preotesiu, F., Jacota, G., Preotesiu, E., 1973. Report, the archives of the I.F.L.G.S., Bucharest.

Richards, J.P., 2015. Tectonic, magmatic, and metallogenic evolution of the Tethyan orogen: from subduction to collision. Ore Geology Reviews **70**: 323–345. https://doi.org/10.1016/j.oregeorev.2014.11.009

Săndulescu, M., 1984. Geotectonics of Romania (in Romanian). Editura Tehnică, Bucharest.

Schmid, S.M., Bernoulli, D., Fügenschuh, B., Matenco, L., Schefer, S., Schuster, R., Ischler, M.T., Ustaszewski K., 2008. The Alpine-Carpathian-Dinaridic orogenic system: correlation and evolution of tectonic units. Swiss Journal of Geosciences, **101**: 139–183. https://doi.org/10.1007/s00015-008-1247-3

Todiriţă-Mihăilescu, V., 1973. Contributions to the study of Cretaceous deposits from the north-eastern flank of Vanturarita Ridge (in Romanian). Analele Universităţii Bucureşti, **22**: 89–98.

Udubaşa, G., Hann, H.P., 1988. Shear-zone related Cu-Au ore occurrence: Valea lui Stan, South Carpathians. Dări de Seamă Institutul de Geologie şi Geofizică, **72–73/2** (1985, 1986): 259–282.

Youngson, J.H., Craw, D., 1999. Variation in placer style, gold morphology and gold particle behavior down gravel bed-load rivers: an example from the Shotover/Arrow-Kawarau-Clutha River system Otago, New Zealand. Economic Geology, **94**: 615–634. https://doi.org/10.2113/gsecongeo.94.5.615

Wierchowiec, J., Mikulski, S.Z., Zieliński, K., 2021. Supergene gold mineralization from exploited placer deposits at Dziwiszów in the Sudetes (NE Bohemian Massif, SW Poland). Ore Geology Reviews, **131**: 104049. https://doi.org/10.1016/j.oregeorev.2021.104049

APPENDIX 1

Field Observations

The fieldwork was concentrated in seven panning locations (sampling sites) as shown in Figure 1, and detailed further. Panning location #1 is on the Olănești River, downstream from the junction with the Cheia River; panning location #2 is at the junction between the Olănești and the Cheia River; and panning location #3 is on the Cheia River upstream from the junction. Sampling site #4 is on an unnamed tributary creek of the Olănești River. Sampling site #5 is on the Câinelui Stream, a tributary creek of the Olănești River, and panning location #6 is on an unnamed tributary creek of the Câinelui Stream. Most of the gold grains were found in location #3, while locations #5 and #7 yielded only one gold grain each.

The distance between the lowest altitude point (location #1) and the highest altitude point (location #7) on the Olănești River is 21 km and the height difference is ~400 m, the gradient being 1.90%. The elevation and the coordinates for each location, and the approximate distance between the panning locations and the Valea lui Stan ore deposit, are given in Table SM1.

Table SM1
Google Earth elevation and coordinates of the panning locations
and the approximate distances to the Valea lui Stan ore deposit

Location	Elevation (ASL)	Coordinates
#1	+296 m	45°07'19"N 24°16'58"E
#2	+353 m	45°09'18"N 24°15'05"E
#3	+396 m	45°10'21"N 24°13'40"E
#4	+477 m	45°11'33"N 24°14'54"E
#5	+698 m	45°16'00"N 24°11'02"E
#6	+813 m	45°17'03"N 24°10'30"E
#7	+695 m	45°15'51"N 24°09'11"E

Panning location #1

Panning location #1 is situated downstream from the junction between the Cheia and the Olănești rivers, being topographically the lowest point in our study (Fig. SM1a). The river flows over a thick bedload of gravel and sand and has a width of ~75 m. The alluvial deposits include clasts of metamorphic rocks (quartzite, amphibolite) and sedimentary rocks (sandstones and limestones). The bedrock is not exposed.

Local seekers after gold at this location use homemade sluice boxes (Fig. SM1a).

Panning location #2

Panning location #2 is at the junction between the Olănești and the Cheia rivers (Fig. SM1b). The river flows over a bedload of gravel and sand which, however, is thinner than at location #1; the bedrock is locally exposed, and is composed of interbedded marls and sandstones.

The lithology of the alluvial deposits is the same as at location #1 with the exception that larger boulders occur on the river banks.

Panning location #3

Panning location #3 is on the Cheia River, upstream of the junction of the Cheia and Olănești rivers. The river flows over or near the bedrock and is up to 10 m in width (Fig. SM1c). The alluvial deposits consist of gravel and sand and contain large boulders up to tens of centimetres in diameter (Fig. SM1d). The boulders are mainly of sandstone and limestone, with subordinate metamorphic clasts. The bedrock consists of marl sequences with a dip of 45° to the south and interbedded sequences of marl and sandstone with a similar dip to the south (Figs. SM1d and SM1e).

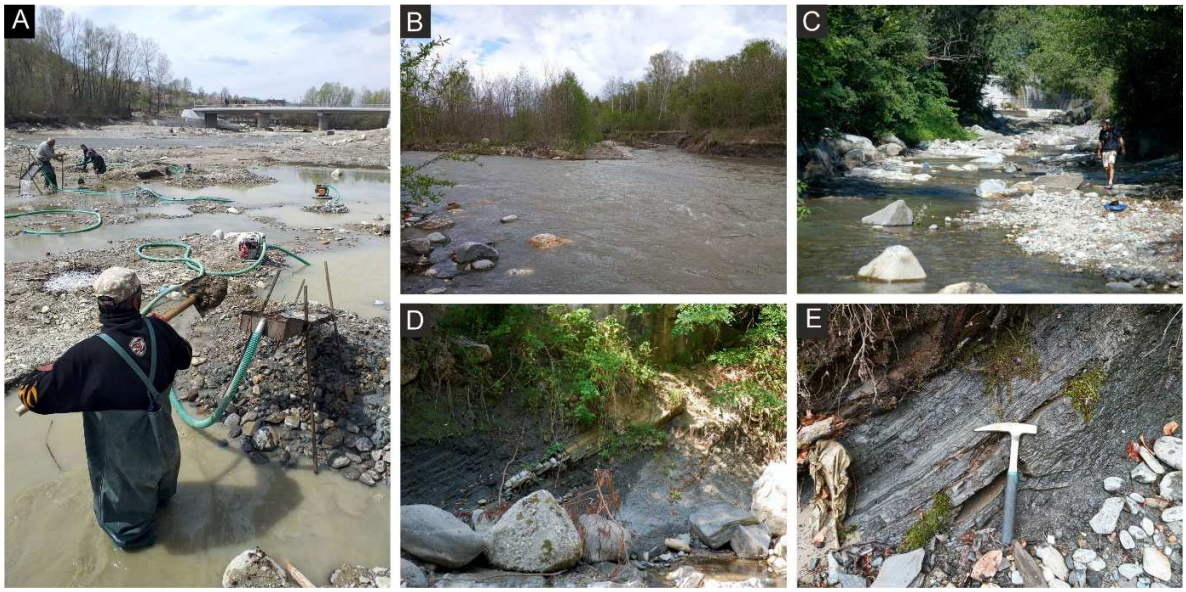

Fig. SM1. Panning locations #1 to #3

A – Panning location #1, which shows local gold-seekers using homemade sluice boxes; **B** – upstream view of the junction between the Cheia River (left) and the Olănești River (right) at panning location #2; **C** – Image of panning location #3, showing the river flowing on or near the bedrock; **D** – Panning location #3 with several boulders deposited on the side of the river; the bedrock consists of interbedded layers of marl and sandstone dipping at 45° dip to the south; **E** – the bedrock of panning location #3 with marl sequences dipping 45° to the south; detail of the exposure shown in Figure SM1d

Panning location #4

Panning location #4 (Fig. SM2a) is situated on an unnamed tributary creek of the Olănești River located upstream from the junction between the Olănești and Cheia rivers.

The creek is seasonal and flows only in rainy periods as a torrent having a width of 1–2 metres. Large boulders over 1 m in size are deposited along the creek together with smaller boulders of limestone and metamorphic rocks.

Panning location #5

Panning location #5 is on the Câinelui Stream, which flows into the Olănești. The river at this location is narrow, having a maximum width of 5 metres (Fig. SM2b), and flows on or near bedrock upon a thin bedload of gravel and sand. There are also dm-sized boulders deposited on the sides of, or within, the river. The bedrock comprises sandstones dipping to the south (Fig. SM2c). Along the stream, there are several exposures of sandstone and conglomerate. The OL01-G4 gold grain was panned from this location.

Panning location #6

Panning location #6 (Fig. SM2d) is situated on a tributary creek of the Câinelui Stream, close to location #5. The creek flows from NNE to SSW and has steep sides (Fig. SM2d). The bedrock of the creek comprises sandstone and along the watercourse, this forms small waterfalls, which can be excellent gold traps. Panning location #6 is very close to the Valea lui Stan ore deposit, which is about 4 km to the north, on the other side of the hill (Fig. 1).

Panning location #7

Panning location #7 has the highest elevation from the Olănești River. The river is narrow, a maximum of 4 m in width, and flows near the bedrock and on a thin bedload of gravel and sand (Fig. SM2e). There are cm-sized boulders along the watercourse, which show similar lithologies to those in the previous locations. The bedrock consists of interbedded marls and sandstones dipping south (Fig. SM2f). The OL01-G2 gold grain was observed by the naked eye in this location.

Fig. SM2. Panning locations #4 to #7

A – downstream view of panning location #4 on a tributary creek of the Olănești River, which flows from west to east; B – upstream view of the Câinelui Stream at panning location #5; the watercourse is narrow and the river flows directly on the bedrock; C – image of panning location #5; the bedrock is formed by sandstones dipping to the south; D – downstream view of panning location #6 on a tributary creek of the Câinelui Stream, with a sandstone bedrock; E – downstream view of panning location #7; F – detail of the bedrock of panning location #7, which consists of interbedded layers of marl and sandstone dipping to the south.